COMPUTER METHODS AND PROGRAMS IN BIOMEDICINE 105 (2012) 217–232

journal homepage: www.intl.elsevierhealth.com/journals/cmpb

Simulation of the human TMJ behavior based on interdependent joints topology

Marta B. Villamil[a,b,*], *Luciana P. Nedel*[a], *Carla M.D.S. Freitas*[a], *Benoit Macq*[c]

[a] *Instituto de Informática, Universidade Federal do Rio Grande do Sul, Porto Alegre, Brazil*
[b] *Applied Computing Graduate Program, Universidade do Vale do Rio dos Sinos, São Leopoldo, Brazil*
[c] *Communication and Remote Sensing Laboratory, Université catholique de Louvain, Louvain-la-Neuve, Belgium*

ARTICLE INFO

Article history:
Received 22 October 2010
Received in revised form
16 May 2011
Accepted 22 September 2011

Keywords:
Temporomandibular joint
Computer Simulation
CT images
MRI images

ABSTRACT

The temporomandibular joint (TMJ) is one of the most important and complex joints of the body and its pathologies affect a great percentage of the human population. The simulation of the TMJ behavior during opening, closing and chewing movements can be very useful to the understanding of this articulation by physicians, helping them to prevent or fix problems due to accidents or diseases. This work proposes a model to simulate the human TMJ behavior based on the concept of two interdependent joints. The model was conceived using multimodal information acquired from CT and MRI images of a live person, as well as motion data acquired from this same person with a magnetic motion capture device. Simulation of movement of other TMJs, based on different morphology of bones and teeth, is obtained by adapting the regular captured motion data through collision detection and treatment methods. The proposed model was evaluated through image registration techniques by comparing our simulated results with real, captured motion data. We also validate the model showing how it can be used to predict TMJ behavior in the presence of different – normal or abnormal – bones and teeth morphologies.

1. Introduction

Anatomy-based modeling of joints is still a challenge in virtual human animation with applications ranging from realistic representation for simulation of different situations to functional anatomy teaching, medical training, and computer-assisted surgery planning [1]. The precise characterization of joint kinematics is essential to understand the function of any articulation. Moreover, human joints normally move along different paths at the internal and external extremities of the bone (the internal one being the proximal extremity to the joint).

The temporomandibular joint (TMJ) is one of the most complex joints of the human body. Its pathologies affect a great percentage of the human population, causing a variety of symptoms. The challenge of simulating this joint is due to its paired nature, since it is composed by two joints linking the motion of one side of the mandible to the other (here called right TMJ and left TMJ). The constraints due to TMJ ligaments and different muscles action cause the mandible to perform complex movements during the normal opening/closing of the mouth. Contractions of various muscles with different shapes and sizes guided by the two articular surfaces make the kinematics and the mechanical environment of this joint not well understood [2].

* *Corresponding author at*: Universidade do Vale do Rio dos Sinos, Av. Unisinos, 950, São Leopoldo, RS 93022-000, Brazil. Tel. +55 51 3591 1122x1636; fax: +55 51 35908162.
E-mail addresses: mbvillamil@unisinos.br (M.B. Villamil), nedel@inf.ufrgs.br (L.P. Nedel), carla@inf.ufrgs.br (C.M.D.S. Freitas), Benoit.Macq@uclouvain.be (B. Macq).
0169-2607
doi:10.1016/j.cmpb.2011.09.010

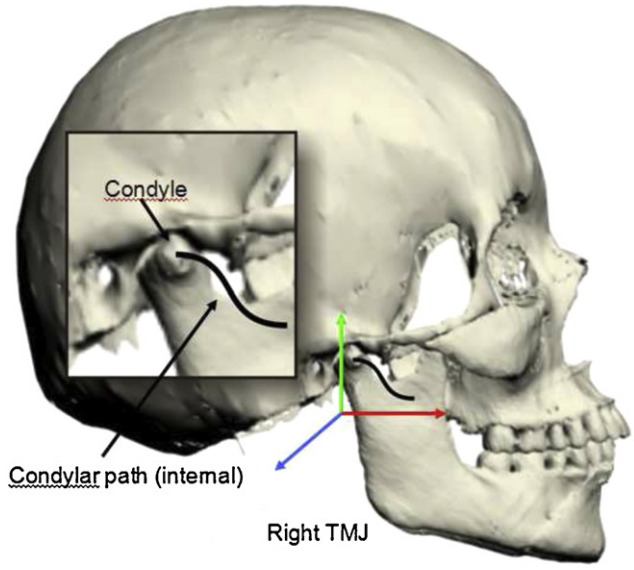

Fig. 1 – The condyle center slides along the TMJ internal path. TMJs are represented by a reference frame with its origin oftenly located outside the mandible bone.

In the initial phase of the opening cycle, the movement is primarily rotational, but after approximately the first 20 mm of jaw opening, the main motion turns into a combination of both translations and rotations. The mandibular condyle (Fig. 1) is able to move almost freely in the three-dimensional half-space bounded superiorly by the articular surface of the temporal bone. Furthermore, if both joints are assumed to be connected rigidly through the mandibular bone, the rotation of the lower mandible around an antero-posterior axis is restricted. In this (simplified) situation, it is able to move with two rotational degrees of freedom (DOFs). Otherwise, if the TMJs are assumed to maintain articular contact all the time, and the joint contact is assumed to be rigid, a translation of the condyle in a direction perpendicular to the articular surface of the temporal bone is restricted, and the number of degrees of freedom for condylar translation is also two [3].

Any condition – normally pathologies and fractures – that prevents the normal translation of one condyle will not prevent the contralateral condyle from sliding forward normally. The result is a deviation of the chin towards the affected side. The mandible asymmetric movements lead to different condylar paths. However, since both condyles are part of the same rigid mandible, their motion patterns are not independent. Moreover, the centers of both condyles slide along curved paths, the so called condylar paths [4]. Studies on subjects with asymptomatic TMJs show that during jaw opening/closing the total rotation around the axis is $24.3^\circ \pm 4.21^\circ$, the translation along it 0.9 ± 0.7 mm, and its distance from the condyle 48.9 ± 9.9 mm [5]. This indicates that the origin of the axis of rotation is never located inside the condyle but often outside the mandible (see Fig. 1). Furthermore, the rotation axis pathways fluctuate only slightly; they are smooth and vary individually.

This work reports our results on building a model of the TMJ based on data acquired from individuals through computerized tomography (CT), magnetic resonance imaging (MRI) and magnetic motion tracking devices. Our model intends to support tailored simulations of TMJs, which would allow the correct treatment and planning of prostheses, yielding fast and effective results.

The remainder of the paper is organized as follows. Next section briefly describes some basic concepts and related works. Section 3 presents the TMJ modeling process, while Section 4 covers the analysis of the proposed model. In the last section we draw our conclusions and comments on ongoing and future work.

2. Background and related work

2.1. *Description of the TMJs motion*

The medical literature describes the motion of TMJs based on many different methods, including simplifications as: the use of roll, pitch, and yaw angles [6], instantaneous center of rotation [7–10], kinematics center [11], helical axis [5,11–13], and non-orthogonal floating axis system methods [14]. All of these works only deal with the capture and analysis of the jaw motion, without formalizing a model that aims at simulating motion with different bones morphologies.

The instantaneous center of rotation (ICR) is typically computed from discrete displacements of at least two points measured on the moving body [7,9,10]. Increments in body movement result in a group of points formed by the corresponding loci of ICRs. Information obtained by the ICR method can be used to determine whether a body motion is pure rotation. If so, the method can be used to determine the location of the true rotation center. The ICR method can also be used to approximate the path of a moving body if the increments are small, in which case the incremental steps are represented by arcs.

There is a controversy about the location of the jaw ICR [15]. Some authors state that there is no consistent location [19,20,8]; others locate the ICR (1) at the top of the condyle [7]; (2) at the mastoid process [16]; (3) at the neck of the mandible [17]; and (4) on a curve that was distant from the mandibular condyle [18]. Two reasons for this diversity of views can be attributed to measurement errors of the different kinds of motion capture devices or the deformation of the skin where the sensor is attached.

Our study uses the ICR concept to calculate only the initial TMJs center of rotation because it has an important limitation to the TMJs case: ICR location is independent of increment size, if, and only if, the actual movement is pure rotation. Previous studies only aimed at defining the TMJs instantaneous centers of rotation at varying points during jaw movement. They are not adequate to quantify motion parameters based on a fixed center of rotation or when movement is composed by relative contributions of rotations and translations. Thus, the motion of the mandible is a complex motion that cannot be easily determined in terms of pure hinge axis rotation.

Two significant improved methods were provided by the helical axis (HA) and non-orthogonal floating axis system. The helical axis or screw axis is a mathematical model which can be used to describe comprehensively the movements of

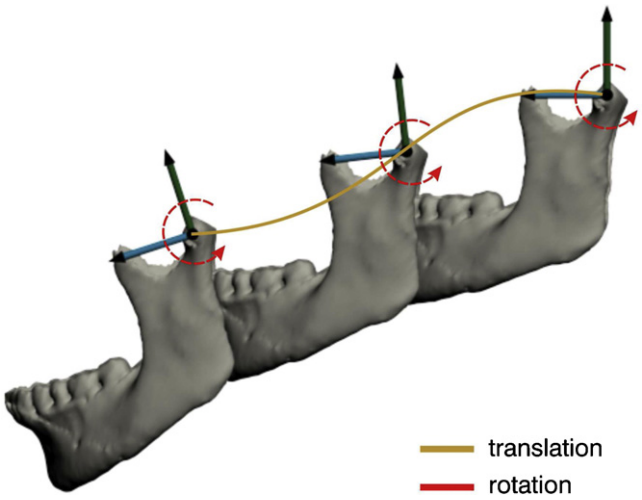

Fig. 2 – Jaw rotations are around axes which intercept the axis of translation.

a rigid body [21] and is frequently used in biomechanics to model joints function [22–24]. If one knows the orientation and position of the helical axis, one can calculate the motion of any point of the rigid body. Although the helical axis method expresses the spatial motion of a rigid body as the combination of a translation along an axis in space and a rotation around it, it has been used to study in-vivo mandible displacements [5,11–13]. The controversial point about TMJ modeling with HA is that the more significant jaw rotations are not around axis of translation but they are around axes which intercept the axis of translation (see Fig. 2).

Leader et al. [14] represented mandibular kinematics using a non-orthogonal floating axis joint coordinate system based on 3D geometric models. Kinematic data captured by an optical motion capture device were registered with the 3D geometric model based on MRI images. Lemoine et al. [2,39] developed a geometry-based algorithm for predicting in vivo mandibular movements. They acquired data using a 3D optical tracking system and sagittal radiographs, and validated the algorithm by predicting the mandibular movement on a cadaver and in a living subject.

All previous authors described jaw motion based in one single joint. To represent the counterbalanced motion between TMJs right and left and to better fit the model to pathological TMJ patients, where one joint works better than, and in a different way, from the other, our work represents TMJs as separated coordinated systems that are interconnected, i.e., motion of one affects the other. The joint internal motion is inferred by using inverse kinematics and bones collision detection and avoidance. In this way, the model can be fit to the data of patients with different bone and teeth morphology.

2.2. *Models of joints*

Introducing individual characteristics based on real data and accurate anatomically based complexities of real joints to the traditional hierarchy of joint transformations can lead to improved realism in human character animation. Many works present different human joints modeling trying to incorporate some complexities and restrictions of real joints.

In biomechanics, a single joint is usually represented by a set of non-orthogonal, arbitrary axes of rotation [25], which can be easily adapted to model human articulations. For example, to model the shoulder joint it is necessary to consider the closed loop consisting of the clavicle, scapula and thoracic surface of the rib cage, which creates a coupling among all these bones. Maurel and Thalmann [26] developed a model where the scapula is linked to the thorax by a 5-DOFs joint (three rotational and two translational), while the other three shoulder joints are 3-DOFs joints.

Other structures also exhibit a high degree of coupled behavior, like the human spine with the tightly coupled vertebrae. Monheit and Badler [27] exploited this fact to develop a kinematics model of the human spine that exhibits flexion/extension, lateral bending and axial twist rotation. Later on, Lee and Terzopoulos [28] introduced a biomechanical model of the human head–neck system. Emulating the relevant anatomy, that model was characterized by appropriate kinematics redundancy (seven cervical vertebrae coupled by 3-DOF joints).

Regarding the three-dimensional (3D) modeling of specific motion involving the mouth opening and closing, Enciso et al. [29] proposed a method which applies 3D motion data obtained from an ultrasonic motion tracker to the segmented mandible of a craniofacial model reconstructed from a CT sequence. To capture the mandible movement they used ultrasonic sensors attached to a head-frame and emitters firmly attached to the mandibular dentition. The advantage of this system was that it was non-invasive, easy-of-use, and provided 3D motion capture in real-time.

Fushima et al. [30] reconstructed the TMJ based on real kinematics data to analyze specifically the TMJ intra-articular space variation during mastication. The reconstruction of the anatomy of the joint was based on tomographic data, while the real movement was recorded with a non-invasive tracking device. These two works [29,30], however, do not provide a general model capable of supporting the study and simulation of this complex joint in different situations.

Recently, Celebi et al. [31] developed a mandibular motion simulator for total joint replacement using a human cadaver head. Two sets of tracking balls were attached to the forehead and mandible, respectively. The cadaver head was then dissected to attach the muscle activation cables and mounted onto the TMJ simulator. The main purpose was the creation of a methodology for re-creating TMJ kinematics in a cadaveric model and analyzing the movement in the computer before and after total TMJ replacement.

General models intended to represent the complex behavior of joints in articulated figures were presented by Maciel et al. [32] and Shao and Ng-Thow-Hing [33]. In both works, joints are represented in a tree topology, where the position and orientation of the joint can interfere in the motion ranges of other joints. Also the axes of their frames can slide along a curve during rotations. Both situations are often present in the kinematics of real anatomic joints.

In the model developed by Maciel et al. [32], every joint in the tree hierarchy has its own reference frame represented by a 4×4 homogeneous matrix called LIM (Local Instance

Matrix), which establishes the relationship between the joint and its parent joint. The root of the hierarchy is the Global Reference Frame. The motion of each joint is defined by entities that represent their translational and rotational DOFs: to each such DOF corresponds a DOF-entity. Each DOF-entity is, in fact, a Local Reference Frame also represented by a 4×4 homogeneous matrix (LIM_{dof}). Geometric primitives or polygonal meshes can be associated to any joint in the hierarchy by means of a LIM_{object}. A generic joint is able to describe any kind of relative motion between two or more adjacent segments of the body. Such motion can be given by: (a) a rotation around one axis; (b) a composed rotation around two or three axes; (c) a translation in one to three axes directions; (d) rotations associated to translations; and (e) a rotation around a sliding axis. Each joint is controlled by a number of such entities, which control the motion of the segment.

Although a tree hierarchy does not fit to the TMJ topology, we adopted the model proposed by Maciel et al. due to the possibility of adapting it to the case of two interconnected joints [34]. Next section presents our temporomandibular joint model based on a new topology characterized by interdependent behavior between two joints.

3. TMJ model

Our temporomandibular joint model consists actually of a pair of joints with three rotational and three translational DOFs each, controlling together the movements of only one bone, the mandible. Movement restrictions are due to bones collision and joints topology (motion of one joint interferes in the adjacent one). Each joint has its own reference frame but its behavior, in terms of rotation and translation, is also dependent on the adjacent joint. The condyles describe an internal (condylar) motion path.

The TMJ reference frames provide the position and orientation of the geometric object representing the mandible. Geometric models of the teeth, and bones of the cranium and mandible were extracted from CT scanning of a volunteer without TMJs pathologies [35]. Real motion data were needed to analyze and model the behavior of the TMJs and to understand how the morphology of the bones and teeth influence the function of TMJs.

3.1. *Interdependent joints topology*

The temporomandibular joint is actually composed of two joints – $\mathbf{TMJ}_{left}$ and $\mathbf{TMJ}_{right}$ – with an interdependent relationship between them (Fig. 4). It means that both are responsible for moving the same bone, the mandible. In this way, a tree topology – typically used to model virtual humans where each graphic object representing a bone is child of a single joint – is not appropriate to the TMJ case. Another method could be the continuously interchange of parenthood relationship between mandible and TMJs (Fig. 3a). In this topology, the parent of the mandible graphic representation would alternate between left and right TMJs during each motion step. But this kind of topology becomes inappropriate too. When one joint (say the left TMJ, for example) (Fig. 3b) controls the motion, the mandible is positioned and oriented related to it. However, when the motion control alternates to the adjacent TMJ (the right one), the inverse happens, and the mandible is positioned and oriented in relation to the right TMJ (Fig. 3c). The previous mandible position is not maintained when there is a transition from motion step *b* to motion step *c*. However, the mandible must always rotate from its previous position independently if the joints alternate in guiding its motion. See Fig. 3f, where each mandible motion step keeps the last position as the origin (Fig. 3e) of the next movement. This topology resembles a 'walking' pattern while performing only rotations.

In our interdependent joints model, $\mathbf{TMJ}_{left}$ and $\mathbf{TMJ}_{right}$ are represented by two reference frames described by two vector basis ($\mathbf{B}_{left}$ and $\mathbf{B}_{right}$) and two origin points ($\mathbf{O}_{left}$ and $\mathbf{O}_{right}$) (Eqs. (1) and (2)). The $\mathbf{O}_{left}$ and $\mathbf{O}_{right}$ are positioned in the Global Reference Frame (**GRF**). Mandible orientation and position related to **GRF** are controlled by transformations represented in a Global Instance Matrix (**GIM**), which deals with the counterbalanced motion between left and right TMJs. Each new $\mathbf{GIM}_{mandible}$ is simply obtained through the multiplication of the old $\mathbf{GIM}_{mandible}$ by $\mathbf{B}_{left}$ or $\mathbf{B}_{right}$, depending on which is in charge of the movement (Eqs. (3) and (4)). Initially, $\mathbf{GIM}_{mandible}$ is the identity matrix. After rotations, $\mathbf{GIM}_{mandible}$ continues to represent a rotation since the arbitrary product of rotation matrices is itself a rotation matrix.

$$\mathbf{TMJ}_{left} = \mathbf{TMJ}_{left}(\mathbf{O}_{left}, \mathbf{B}_{left}) \tag{1}$$

$$\mathbf{TMJ}_{right} = \mathbf{TMJ}_{right}(\mathbf{O}_{right}, \mathbf{B}_{right}) \tag{2}$$

$$GIM\prime_{mandible} = \mathbf{B}_{i} \times \mathbf{GIM}_{mandible} \tag{3}$$

$$\mathbf{B}_{i} = \mathbf{B}_{left} \text{ or } \mathbf{B}_{i} = \mathbf{B}_{right} \tag{4}$$

When the mandible bone moves based on one of the TMJs, the origin of the adjacent TMJ also moves. For example, if the movement at a certain instant of time is a rotation around an arbitrary vector of $\mathbf{TMJ}_{right}$, the origin of $\mathbf{TMJ}_{left}$ is updated as in Eq. (5).

$$O\prime_{left} = \mathbf{B}_{right} \times \mathbf{O}_{left} \tag{5}$$

Fig. 4 shows an exaggerated representation of mandible motion along three time steps. Fig. 4a shows a mandible at the initial position when $\mathbf{GIM}_{mandible}$ is the identity matrix. When a rotation around a vector $\boldsymbol{u}$ is applied to $\mathbf{TMJ}_{right}$ (Fig. 4b), the origin of the adjacent joint ($\mathbf{O}_{left}$) and the mandible also rotate around the same axis. At the next motion step (Fig. 4c), another rotation is applied, this time around a vector $\boldsymbol{v}$ of $\mathbf{TMJ}_{left}$. The control of the mandible motion changes as well as the origin of $\mathbf{TMJ}_{right}$ ($\mathbf{O}_{right}$) and the mandible rotates around $\boldsymbol{v}$. The old position and orientation of $\mathbf{TMJ}_{right}$ and mandible are kept, and the new motion step is performed from this position. Through this kind of topology the transformations that occur in one TMJ will affect the other one. $\mathbf{GIM}_{mandible}$ always controls the position and orientation of the graphic object which represents the mandible by accumulating the transformations performed by both TMJs.

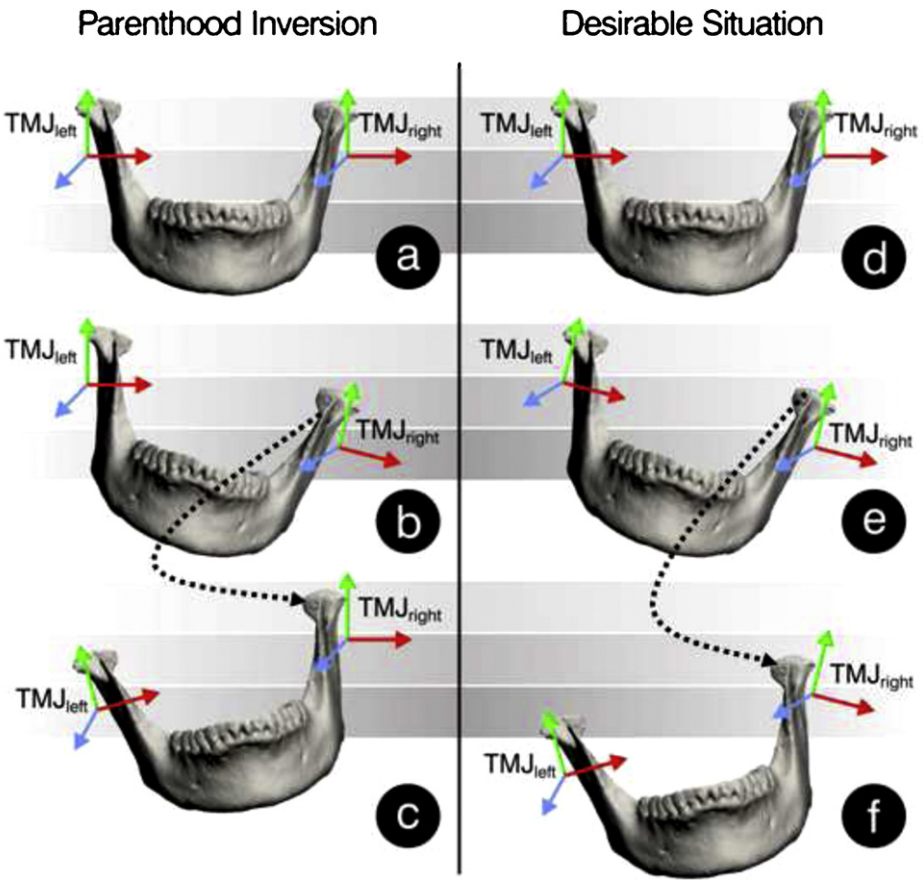

Fig. 3 – Two sequences of mandible movement. The left one (a–c) is based on a simple parenthood inversion. The right one (d–f) is the desirable situation. Rotations have to be performed based on the last mandible position, even if the joint that controls the movement is changed. Dotted arrows indicate that, when motion changes from (b) to (c), TMJ_{right} and mandible returns to their old positions before performing new motion. On the other hand, in the desirable situation, mandible and TMJ_{right} keep their old positions (e) before performing a new motion (f).

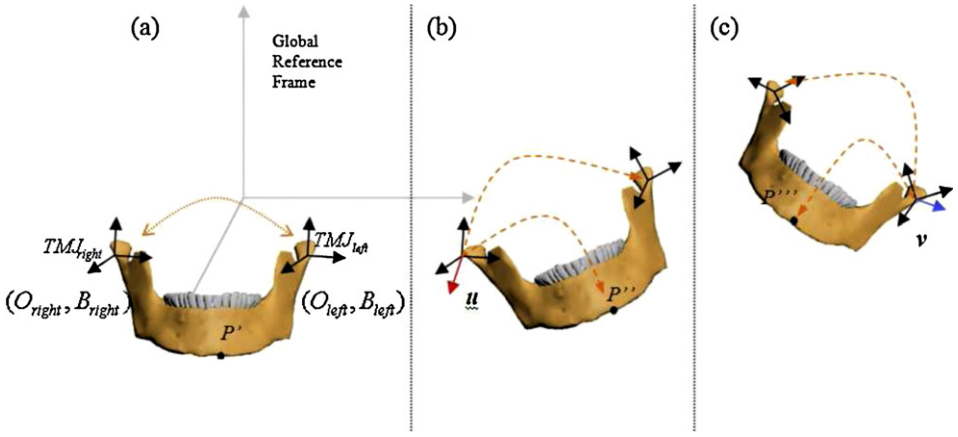

Fig. 4 – Both TMJs have an origin and a vector basis (a). As an example, mandible and TMJ_{left} rotate around a vector u of TMJ_{right} (b). At (c) mandible and TMJ_{right} rotate around vector v of TMJ_{left}. Subsequent mandible and TMJ rotations are always performed based on the last position.

3.2. *Motion model*

The motion model is based on a Catmul-Rom spline that describes the incisal path (i.e., the path followed by a point located between the lower incisive teeth). The curve was derived from a set of real data captured from of a volunteer without any TMJ pathology [35].

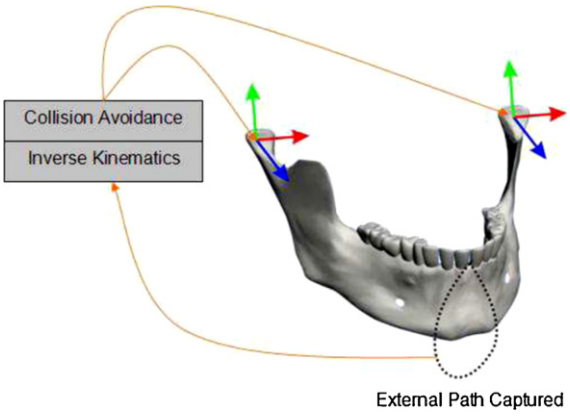

Fig. 5 – Axis and values of magnitude of rotation, and amount of translation are determined from the captured external path using inverse kinematics and collision avoidance.

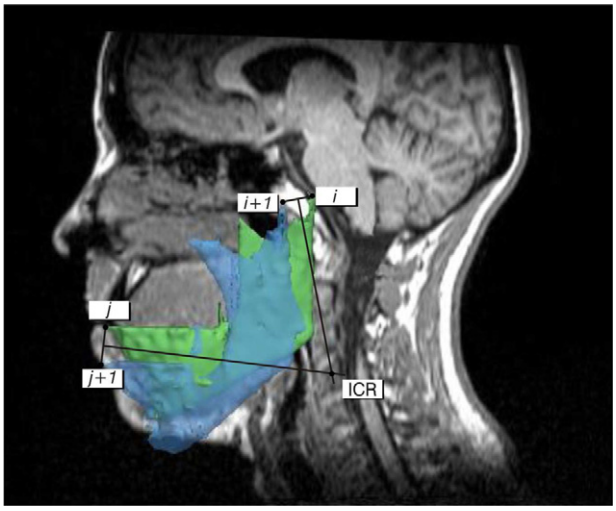

Fig. 6 – Representation of instantaneous center of rotation.

To reproduce the motion of the mandible, we need to infer the internal (condylar) path based on the external (incisal) one. An inverse kinematic method was applied to infer the rotations and translations at each TMJ needed to move the mandible. The set of positions of both TMJs reference frames obtained by this method represents the TMJs internal paths.

Both TMJs in our model have three DOFs of rotation. As any ball-and-socket joint, the TMJs rotation axes are free to change at each time step. It means that their directions are not fixed and can be decomposed into three DOFS. The origins of joints frames are placed at initial ICRs (Section 3.2.1). At each mandible motion step, rotation occurs around a new axis with its corresponding angle of rotation defined by the external motion path and bones collision avoidance (Section 3.2.2) (Fig. 5).

Next sections give details about each component of our model of motion.

3.2.1. *Positioning the initial instantaneous center of rotation*

The instantaneous center of rotation (ICR) method proposed by Lepera [17], sometimes referred to as the 'hinge axis', is often used in joint mechanics analysis to find the center of rotation when a movement is described only by rotations. Jaw movement is primarily rotational only at the first millimeters of opening; so, only the initial ICRs are calculated from input data. After that, the next ICR points will follow the TMJs condylar path, which is obtained from the incisal path and the collision avoidance between the mandible and the cranium bones.

Initial ICRs (for right and left TMJs) were obtained through calculations using fiducial points on dynamic MRI data. The mandible area was segmented on MRI images taken from two different positions of a volunteer: first, with the jaw totally closed, and then with the jaw partially open at two centimeters (Fig. 6). The two anatomical fiducial marks were located at the top of condyles (*i*) and at the center, between the low incisives (*j*).

Consider the movement of these two points (i_t ; j_t) from time t to $t+1$ (i_{t+1} ; j_{t+1}). The ICR for this increment of movement can be calculated by tracing perpendicular bisectors between the lines (i_t) to (i_{t+1}) and (j_t) to (j_{t+1}). The ICR is at the intersection point of the bisectors (Fig. 6).

3.2.2. *Condylar path derivation*

Having obtained the ICRs that determine the starting point of each condylar path, the rest of this path is obtained from inverse kinematics and collision avoidance.

For inverse kinematics, the incisal point is set as end-effector, and each sample point along the Catmull-Rom spline is set as a goal position. The linkage is simple enough for directly calculating joint angles by using an analytical approach as there is only one rigid segment (mandible) connected to TM joints. Cross product between the vector originated at TMJ frame center to the incisal point and the vector from the same origin to the captured point gives the joint axis of rotation (Fig. 7). The angle of rotation is obtained by dot product between these vectors. First of all, mandible rotation tries to reach the goal position. If this is not sufficient, a mandible translation is performed. Translation moves both TMJ's origins and the mandible graphic object. The normal condylar path corresponds to this sequence of transformations. Since the model was derived from a specific normal subject, it would not be valid without fitting to different bones and teeth morphologies. Next section presents the generalization of our TMJ motion model.

3.2.3. *Condylar path and morphology*

The normal condylar path is represented by the sequence of transformations that should be applied to $\mathbf{TMJ}_{left}$ and $\mathbf{TMJ}_{right}$ to move the mandible. Applying the same sequence of transformations to different bones morphology for sure would result in collision between the jaw and temporal bones in the condylar socket.

So, the model is completed by a collision detection and treatment method, to avoid interpenetration of meshes representing the bones of the cranium and the mandible. The

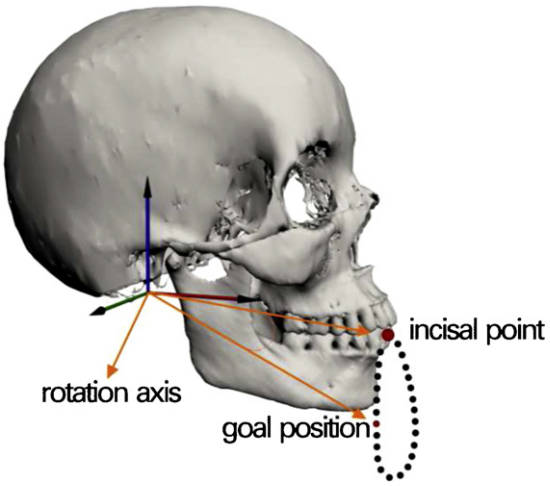

Fig. 7 – Two vectors used to calculate angle and axis of rotation. They are originated at TMJ frame. One points to the incisal point and the other one points to a position along the captured path.

collision detection module uses Oriented Bounding Boxes hierarchies [36] to check, at each motion iteration, if there is a collision. Once a collision is detected, when a rotation is performed, the origin of the reference frames that represent the TMJs should be moved to a point closer to the joint. The cause of this adjustment is that the closer the origin of the rotation axes is to the condyle center, less the condyle will dislocate inside the condylar socket (Fig. 8). This adjustment is accomplished through a sequence of small steps of reference frames displacements until the rotation does not cause collision anymore.

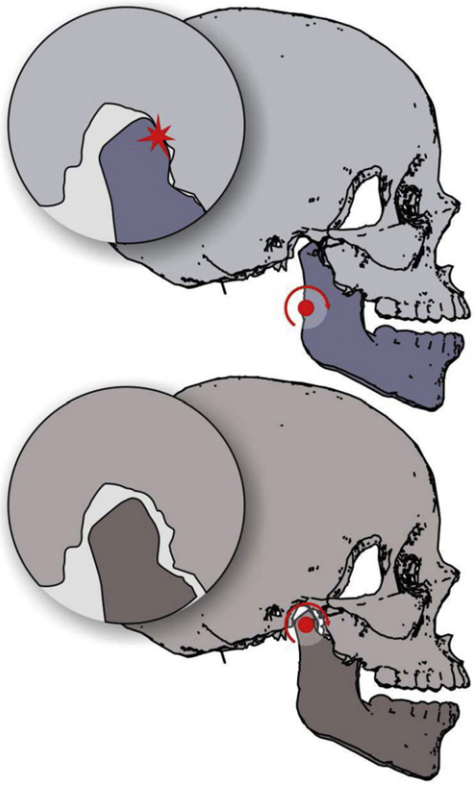

Fig. 8 – If the origin of rotation axis is closer to the condyle center, there will be less collisions between the mandible bone and the condylar socket.

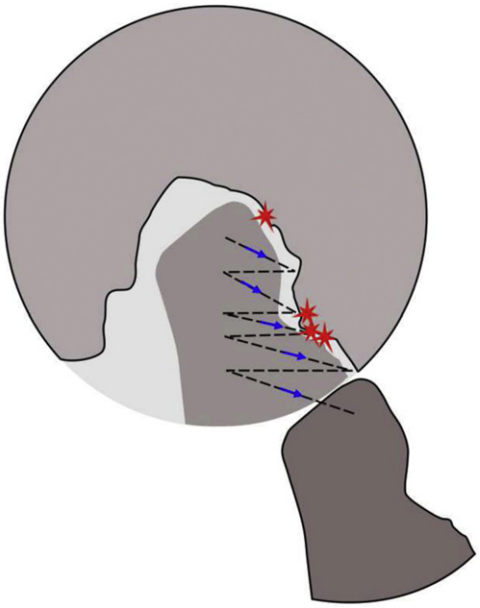

Fig. 9 – The algorithm tries to find another path to the mandible based on the saved path and on collision avoidance.

Otherwise, if a collision is detected during a mandible translation, the algorithm will determine iteratively a different displacement. At first, a shorter translation is tried along the same direction. If a collision is still detected, the algorithm adjusts the origin of the translation in the sagittal plane based on the current TMJ origin and on the collision point (Fig. 9).

4. Discussion

This section discusses the analysis of our TMJ model, which was performed with two main objectives. The first one is related to its verification, i.e., the evaluation of its correctness in relation to the real data used for its proper development, while the second analysis aimed at its validation for evaluation of its applicability to other geometric models (representing different subjects), exactly to prove the hypothesis of the relation between shape and function in this joint.

4.1. *Model verification*

Verification is of vital importance for a model like this to be used in medical applications. It was accomplished through the comparison between the simulated and the real movements of the same subject, as well as through the analysis of the simulated opening–closing movement of the standard, normal TMJ and its comparison against the information in the classical literature.

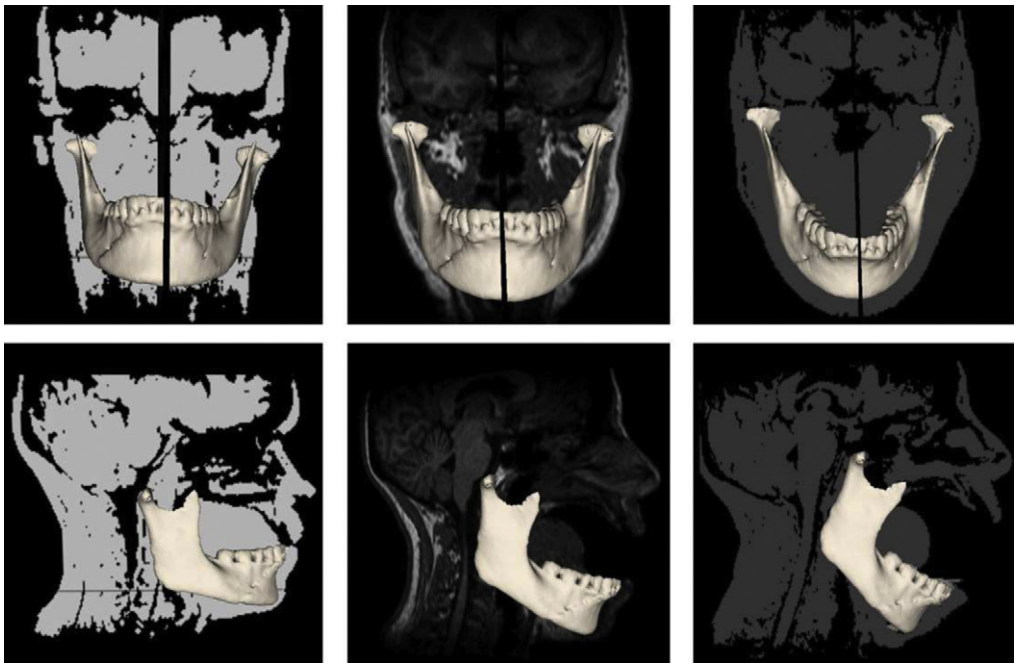

Fig. 10 – Frontal and lateral views of the registration between the jaw region segmented on MRI images, and the corresponding mesh at three different positions extracted from the TMJ model: jaw closed (first column); jaw 2 cm opened (second column); and jaw totally opened (last column).

4.1.1. *Analysis of poses*

In this section we describe the comparison based on a registration process between medical images showing the subject in different poses with the polygon mesh representing the subject's mandible in the simulated analogous poses.

Through an image registration process it is possible to transform the different datasets (dynamic MRI and 3D model at different motion positions) into one coordinate system. A basic image/set of points similarity-based registration method consists of a transformation model, which is applied to a set of coordinates in order to find their corresponding coordinates in the target image space.

For this registration process, three mandible positions were chosen: (a) mouth closed, (b) mouth with one centimeter opening, and (c) mouth with a three centimeters opening. Although CT images would be better to segment bones, this kind of exam is not indicated to capture the movement for a dynamic validation and there is also the problem of high X-ray exposition. So, we used images obtained from dynamic MRI even knowing that these would yield lower quality segmentation. Observing Fig. 10, it can be noticed that jaw edges are not so clear, but the resulting segmentation was enough for the registration process.

We used an image similarity metric that quantifies the correspondence between mesh points and features in image space achieved by a transformation called Match Criterion Value (MCV), and an optimization algorithm that tries to maximize the mesh points and image similarity by changing the transformation parameters. The implementation of Saito's Euclidean Distance Transform [37] found in [38] was applied. The algorithm has an $O(N^{4/3})$ complexity, where N is the number of mesh points.

Table 1 – Matching criterion values after registration. The jaw positions obtained from the TMJ model show a good match with the segmented jaw in MRI images extracted from the volunteer in three jaw positions. First line indicates the ideal result, i.e., registration between the mesh and the same CT images used for its reconstruction.

Registered objects	Accuracy
CT vs. initial mesh jaw 3 cm opened, comparison parameter	0.0013
MRI vs. mesh transformed jaw totally closed	0.2490
MRI vs. mesh transformed jaw 2cm opened	0.1872
MRI vs. mesh transformed jaw 3cm opened	0.0835

The Match Criterion Value transformation [38] gives a quantitative assessment of the registration accuracy. For evaluation purposes, we used the MCV as a result from the registration between the dynamic MRI poses and the set of points extracted from the mandible mesh. It measures how mesh points match with the mandible region segmented on MRI images. We also calculated a MCV between the CT and the mandible mesh as a comparison parameter with the MRI vs. mesh transformed by the model registration to know how good the obtained results were (Table 1). Obviously, registration between the CT and the mandible mesh is the better one because the mesh was extracted directly from CT, but the other results are very close and thus can be considered good for our verification purpose.

4.1.2. *Motion analysis*

This section discusses results related to a set of simulations concerning to the motion of a normal articulation.

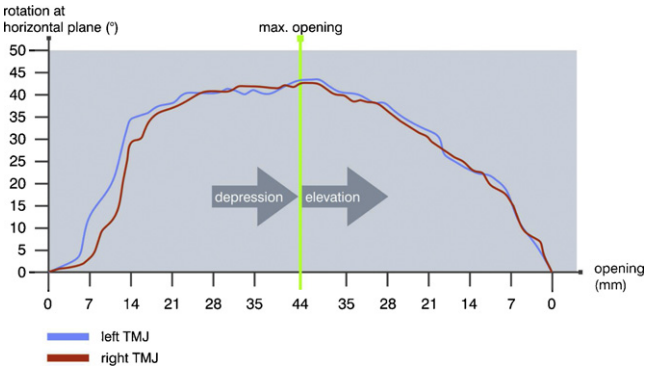

Fig. 11 – Magnitudes of rotations of the jaw on the sagittal plane measured in each TMJ along mouth depression (0–44) and elevation (44–0) movements.

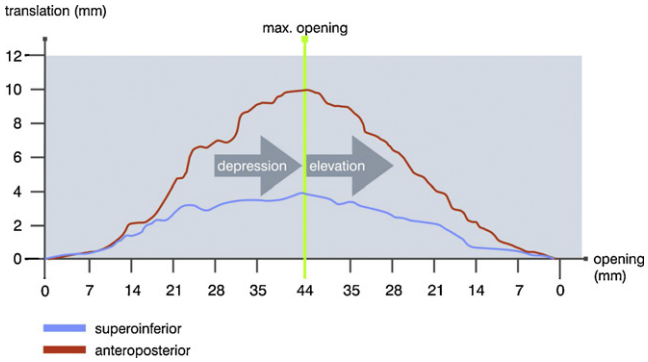

Fig. 13 – Magnitude of translations in the anteroposterior direction (and the opposite) during depression and elevation of the jaw.

As described in Section 3.2.3, our model was developed based on the complete movement (of the incisal point) of the mandible from closed mouth configuration to maximum jaw opening. In this way, we can investigate how shorter movements, as those involved in mastication, for example, influence the TMJ condylar motion. Moreover, we are able to study other relationships like the one between the downward and forward translation of the jaw on its axial plane and the forward translation of the TMJ origin along the condylar path.

For the analysis of the magnitudes of the transformations that the jaw suffers during the opening–closing movement, we captured the incisal pathway from the total closed mouth (0 mm between the incisal point and the inferior part of superior incisive teeth) until total depression of the mouth (44 mm) as well as the pathway of mouth closing (44–0 mm). During this movement, the largest increase of rotation magnitude measured, for the angular displacement on the sagittal plane, was during the first 10 mm of mouth opening. On the other hand, the decrease of the angular displacement during the closing movement is smooth, as shown in Fig. 11. We can also observe a small lateral deviation of the jaw measured by angular displacements (Fig. 12).

A point to be noticed in our work is that although the model was developed from measures taken from TMJs considered normal for medical standards, we cannot compare the motion

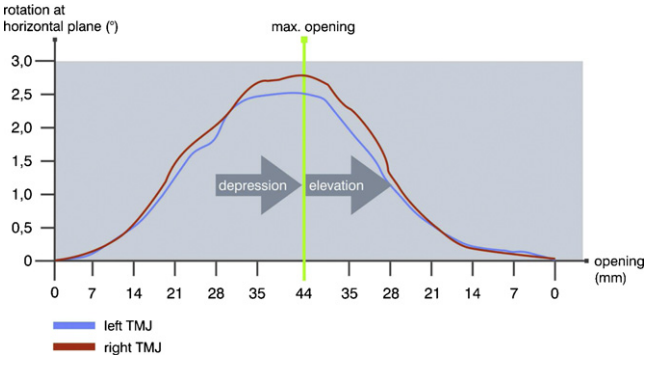

Fig. 12 – Magnitudes of rotations of the jaw on the horizontal plane measured in each TMJ along mouth depression (0–44) and elevation (44–0).

we obtain from our model with the motion of mechanical joints. There is always a small disparity in condylar and maxillar forms between the left and right TMJs as well as different muscular forces applied to each one. Moreover, the condyles do not have the morphology of a perfect cylindrical surface and they differ from each other. Also, the initial centers of rotation of both TMJs are different, and they do not have the same alignment in none of the planes (coronal, axial and sagittal). All these characteristics yield different jaw angular displacements for each TMJ, beyond the lateral displacements that occur during the mandibular depression and the small motion variations demonstrated in Figs. 11 and 12.

During the mandible depression, the more significant contribution of magnitudes of translations are noticed in the anteroposterior and superoinferior directions (Fig. 13) if compared with another type of movement, as in the one of chewing, for example, where there is almost no contribution from translations. The variation in the magnitude of rotations and number of translations that occur during mouth opening if compared with the closing movement confirms the classical comments of Posselt [40] that the jaw covers different pathways during its depression and elevation.

In order to investigate the difference between the captured and the simulated movement for the same patient, we plot both paths in three views: sagittal, frontal and axial. We also chose three different points at similar positions on each path and compared them (Fig. 14): first, at the top of the path in the sagittal view; second, at the bottom and another one, approximately in the center of the path (the blue marks, in Fig. 14). During the opening/closing movement, the maximum difference in their positions were: 4.3 mm (top point), 5.4 mm (bottom points) and 4.75 mm (middle points).

The results presented here in terms of magnitude of translation in the sagittal plane are very similar to the results presented by Lemoine et al. [39]. The incisal point translation recorded by them shows a maximal magnitude of 4 mm in the superoinferior direction and a maximal magnitude of 10 mm in the anteroposterior one. In terms of the magnitude of rotation of the mandible, our work presents almost the double magnitude in comparison with their work. This difference might be due to the fact that we used the ICR method to calculate the initial center of rotation, and its position changes

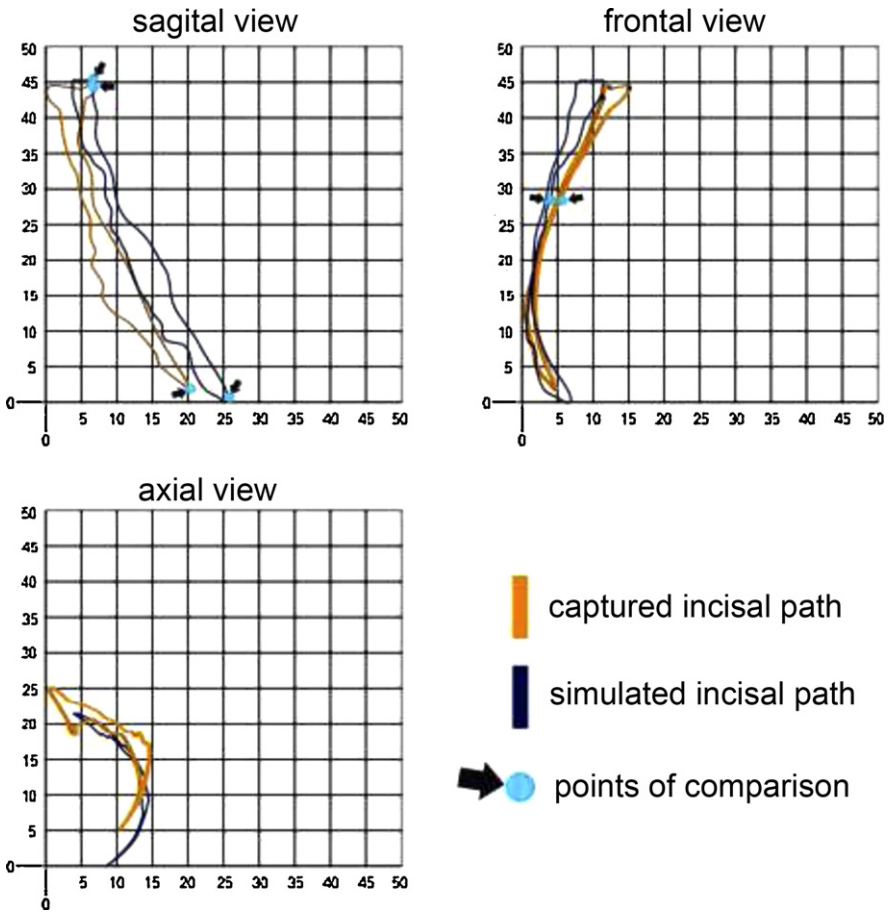

Fig. 14 – Comparison between the incisal path captured and the simulated one.

during the simulation to avoid collision between the condyle and the condylar socket. In their work, Lemoine et al. [39] used the geometric center of the condyle to predict the mandibular movement.

We can also compare our results against the recent work of Celebi et al. [31]. This work shows the simulation of mandibular opening motion at the lower incisor based on cadaver muscle activation. Incisal point at sagittal view performs around 20 mm of displacement at anterior-posterior direction and 45 mm at inferior-superior direction. In terms of lateral displacement it performs 24 mm. It is very closed concerning the incisal point path simulated and captured showed at Fig. 14.

In the next subsection we discuss the validation of the model by applying it to simulate movements of the TMJs with different bone and teeth morphologies.

4.2. *Model validation*

Model validation is concerned to its applicability to the intended purpose. In the case of the TMJ model, we intended to use it in the prediction of the TMJ behavior in the presence of different normal or abnormal bones and teeth morphologies.

To validate the proposed model, it underwent through a second set of analyses where we capture the jaw movements from individuals with different morphologies and compared them to the respective simulated movements. These analyses are described in the following subsections.

4.2.1. *Data acquisition for validation*

An important point in our validation method was the avoidance of new CTs and MRIs in the subjects that volunteered for this analysis. The polygons meshes representing the cranium and mandible of these volunteers were created based on the original mesh we obtained from the subject who has the TMJ without pathologies.

Cephalometric measures of two individuals were used for customyzing the polygonal mesh originally extracted from CT images. The lines observed in the cephalometry are projections, as well as the points of the skull that are projected in the X-Ray image. For registering the projected cephalometric measures to mesh measures, we used two X-Ray examinations (one frontal and another lateral) with its respective cephalometries. The cephalometric measures were extracted from three known analyses: *Frontal of Rickets*, *Lateral USP* and *Macnamara*. The first one is the common frontal analysis obtained from radiology laboratories while the second and third ones are frequently used for diagnosis in maxillofacial orthognathic surgeries. One of the volunteers has a normal TMJ and the second one has a pathological TMJ.

From these analyses we extracted measures of the lines necessary for the adaptation of the basic mesh to obtain

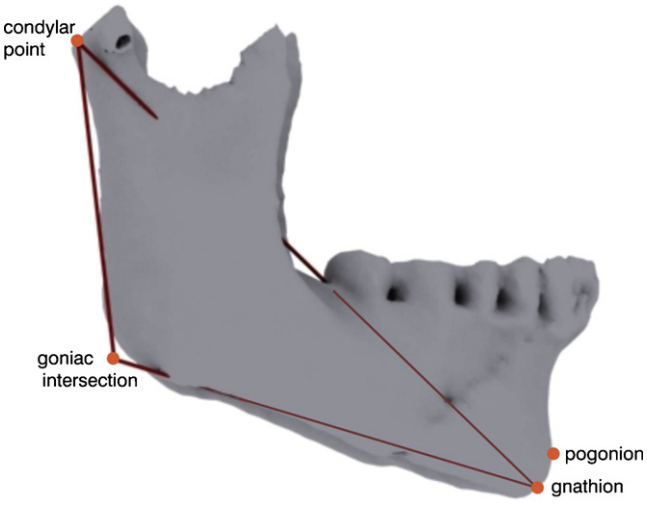

Fig. 15 – Known cephalometric points used to customize the polygon meshes of volunteers from our basic mesh avoiding new CT exams.

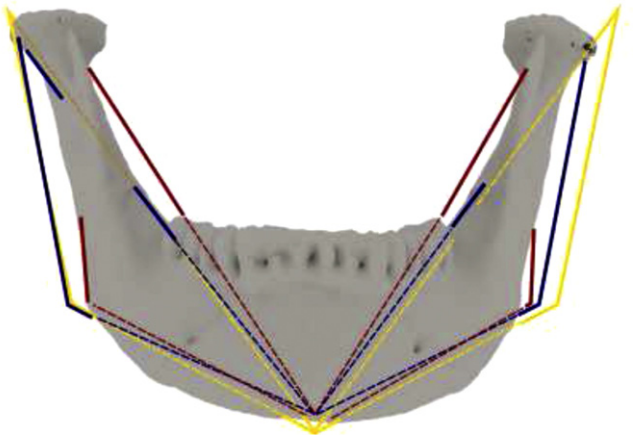

Fig. 17 – 3D cephalometric tracings: red lines represent the measure of original jaw used to construct the model, blue and yellow lines represent the measures extracted from cephalometries of the two volunteers.

models of each volunteer. The lines were traced from four known cephalometric points (Fig. 15):

- Condylar point (CP): maximum posterosuperior point in the contour of the mandibular condyles
- Goniac intersection (GoI): intersection of the mandibular plane with the line that passes through the posterior edge of the mandibular branch
- Gnathion (Gn): maximum anteroinferior point in the contour of the chin bone
- Pogonion (Pog): maximum posterior point in the contour of the chin bone

Other auxiliary measures were also extracted directly from the cephalometric tracings even if they are not used for regular cephalometric analysis. From the original standard (normal) mesh, two new meshes were generated based on the measures described above. The process was carried out through the use of 3DS Max®, following the steps described below:

(1) Some points were marked in the original mesh to serve as basis for the measures in the reconstruction process (Fig. 16(1)).
(2) A triangle was traced linking the goniac intersection, the condylar point and the gnathion in the basic mesh (Fig. 16(2), red lines). We then take the position of the

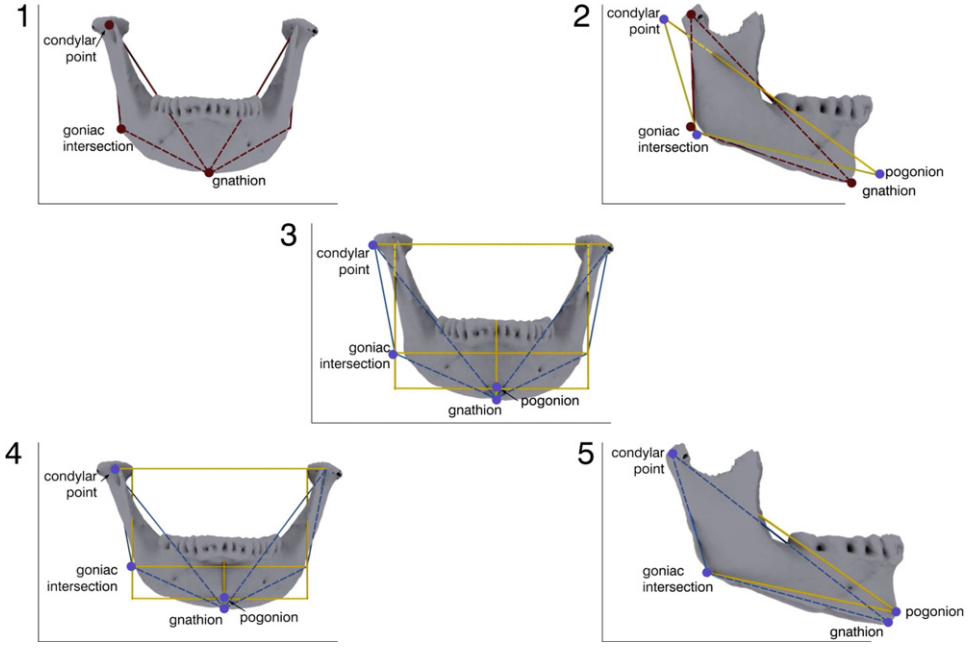

Fig. 16 – The steps to modify a volunteer jaw mesh using measures obtained from cephalometry analyses. The two last figures (4 and 5) present the morphology of the modified jaw.

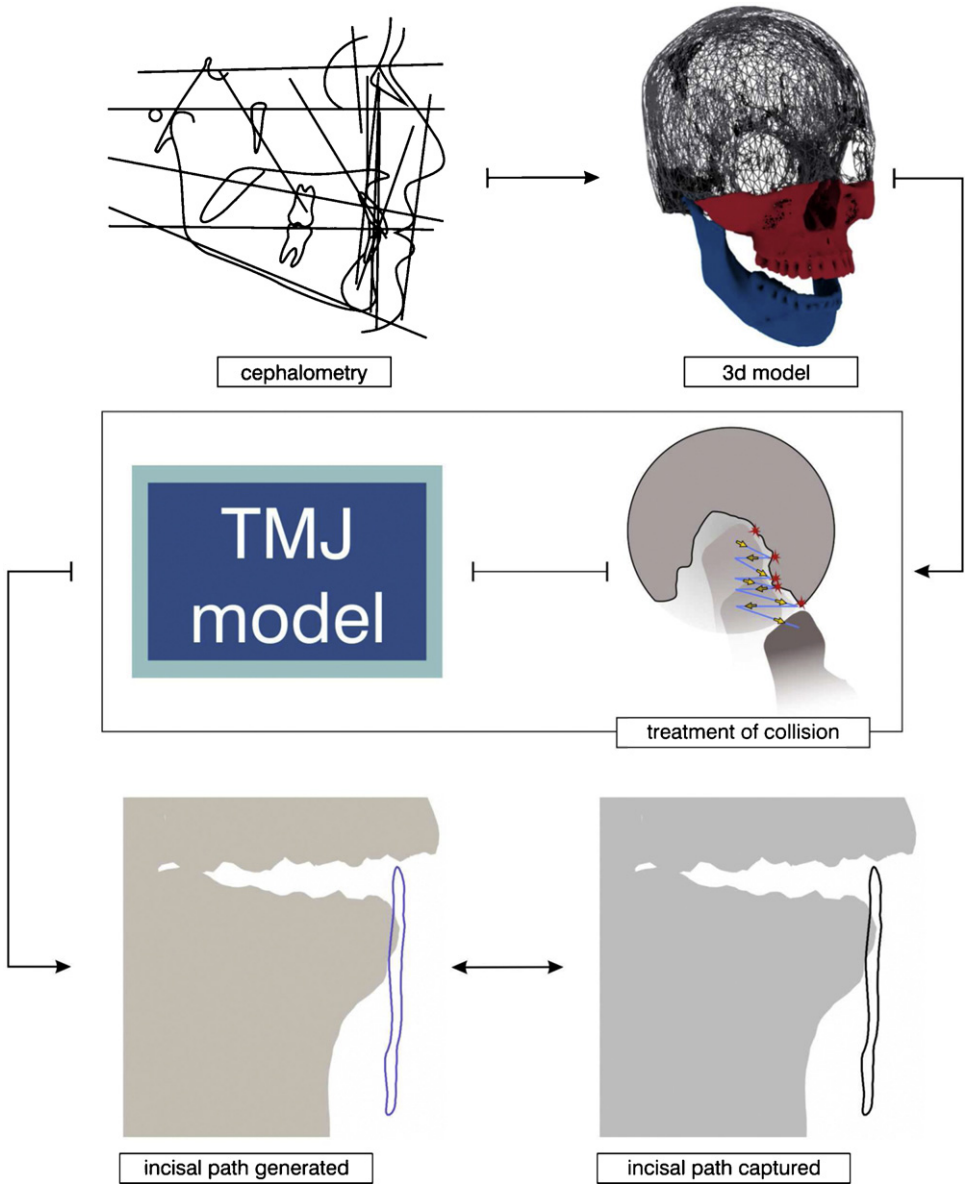

Fig. 18 – For model validation the generated curve must be compared with the real captured curve. The 3D model is modified based on real cephalometric measures (obtained from a volunteer) and put into motion using our model. The skull bones and teeth morphology and treatment of collision can be seen as model parameters.

goniac intersection in the cephalometry of a volunteer, and superimposed it to the goniac intersection previously marked. Moreover, based on the same cephalometry, we traced another triangle composed by the goniac intersection, the pogonion and the condylar points (Fig. 16(2), yellow lines). This triangle was traced in a way that the direction of the line goniac – pogonion, on the sagittal plane was preserved. Adapting the basic mesh to a volunteer mandible model requires adjusting the yellow triangle to the red triangle.

(3) Superimposing the cephalometry frontal view and the basic mesh frontal view allowed us to extract the other measures we need to transform the basic mesh into the volunteer model. The position of the gnathion was obtained from the measure of the superior part of inferior teeth to the inferior part of the chin (Fig. 16(3), yellow vertical central line). The frontal position of the pogonion was also extracted from this same line. The distance between the two goniac intersections was obtained from the measure of the line that links both goniac intersection points (Fig. 16(3), yellow horizontal central line). The same was done between the two condylar points in the frontal plane (Fig. 16(3), yellow horizontal superior line). With these measures, which represent the differences between the points in the basic mesh and the points of a volunteer's mandible (Fig. 16(3), yellow lines), we applied transformations modifying the basic mesh into a volunteer mandible model (Fig. 16(3), blue lines).

Fig. 16(4) and (5) shows the frontal and sagittal views of the modified mesh, respectively.

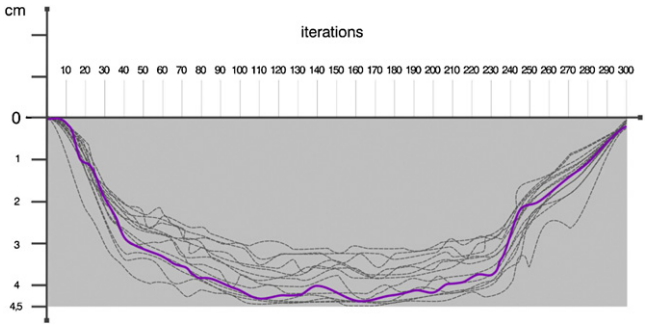

Fig. 19 – Volunteer 1: the points in the sagittal plane representing the captured incisal paths are represented in dotted grey. The points generated by the model in the sagittal plane are represented in magenta. The totality of the generated points is inside the convex hull of the totality of the points of 15 paths captured for validation purpose. (For interpretation of the references to colour in this figure legend, the reader is referred to the web version of the article.)

Fig. 17 presents the simplified jaw measures from three individuals: the blue lines represent the measures of the standard jaw used to generate the model superimposed to the original mesh; the yellow and red lines indicate measures used to generate two other meshes that represent the jaws of the two volunteers used in the validation process. They had their incisal pathways captured to confront with the ones generated by the model when applied to the geometric representation of their cranium and mandible.

Fig. 18 summarizes the whole methodology employed in this validation phase.

4.2.2. *Simulated and acquired motion comparison*

To compare the real movements of the volunteers and the ones generated by the model, we captured their mouth opening–closing movement, i.e., the positions of the incisal point during jaw depression-jaw elevation, in the same way the standard pathway was captured.

We captured 15 incisal point paths for each volunteer, and registered them in the respective geometric representation of the skull of each individual. Then, we simulated the opening–closing movement using the TMJ model for each subject.

The captured and the simulated points of each individual were plotted in the sagittal, axial and frontal planes. The curves from the individual with normal TMJ are plotted in Figs. 19–21 , and the ones from the volunteer with pathological TMJ are shown in Figs. 22–24 . Results show that the incisal

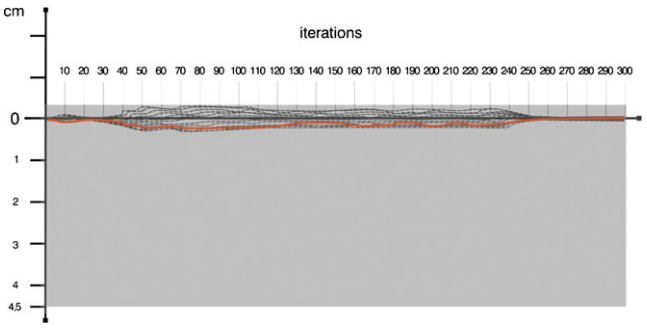

Fig. 20 – Volunteer 1: the points in the axial plane representing the captured incisal paths are represented in dotted grey. The points generated by the model in the axial plane are represented in orange. The totality of the generated points is inside the convex hull of the totality of the points of 15 paths captured for validation purpose. (For interpretation of the references to colour in this figure legend, the reader is referred to the web version of the article.)

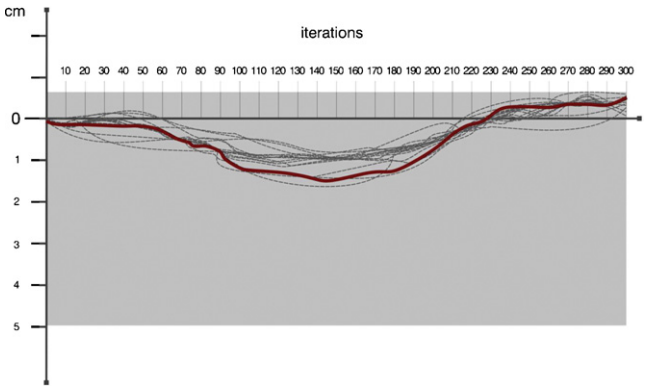

Fig. 21 – Volunteer 1: the points in the frontal plane representing the captured incisal paths are represented in dotted grey. The points generated by the model in the frontal plane are represented in red. The totality of the generated points is inside the convex hull of the totality of the points of 15 paths captured for validation purpose. (For interpretation of the references to colour in this figure legend, the reader is referred to the web version of the article.)

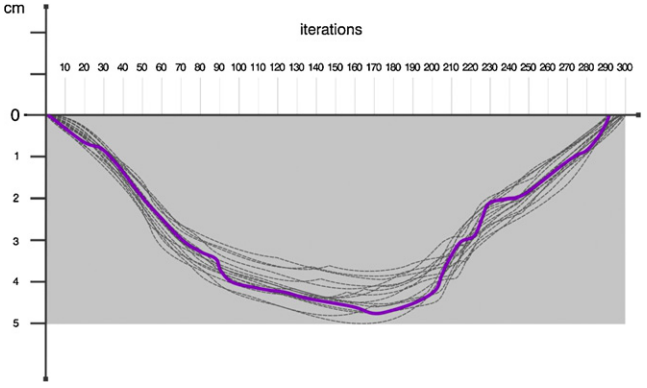

Fig. 22 – Volunteer 2: the points in the sagittal plane representing the captured incisal paths are represented in dotted grey. The points generated by the model in the sagittal plane are represented in magenta. The totality of the generated points is inside the convex hull of the totality of the points of 15 paths captured for validation purpose. (For interpretation of the references to colour in this figure legend, the reader is referred to the web version of the article.)

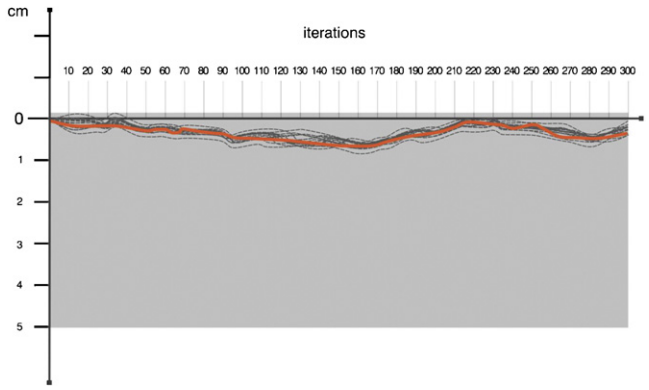

Fig. 23 – Volunteer 2: the points in the axial plane representing the captured incisal paths are represented in dotted grey. The points generated by the model in the axial plane are represented in orange. The totality of the generated points is inside the convex hull of the totality of the points of 15 paths captured for validation purpose. (For interpretation of the references to colour in this figure legend, the reader is referred to the web version of the article.)

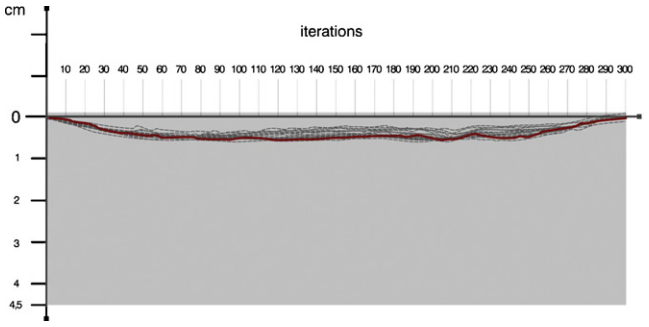

Fig. 24 – Volunteer 2: the points in the sagittal plane representing the captured incisal paths are represented in dotted grey. The points generated by the model in the sagittal plane are represented in red. The totality of the generated points is inside the convex hull of the totality of the points of 15 paths captured for validation purpose. (For interpretation of the references to colour in this figure legend, the reader is referred to the web version of the article.)

point pathway obtained from the model is inside the convex hull of the totality of the points that represent the captured pathways.

Based on the fact that the geometric model was obtained from a standard skull manually adapted with the use of cephalometric measures, we conclude that TMJ model is sufficiently consistent. We suggest that with a more precise geometric model, the simulated movements would be even closer to the real ones.

5. Conclusions

In this paper we introduced a model to simulate the temporomandibular joint behavior of human beings. The TMJ model is based on a joints' topology, which deals with the balanced motion between right and left TMJs useful to simulate pathologies that affect one TMJ in a different way of the other. The TMJ motion model was obtained from real data: CT and dynamic MRI images for 3D model reconstruction and model validation, and a motion path obtained through a magnetic motion capture system. TMJ model was also applied to different mandible morphologies to analyze and compare motion generated by the TMJ model and real mandible movements.

The main contribution of this model is its ability to deal with the complex movement of the TMJ in a simple way, due to its joints topology that takes into account the linking between the right and left TMJ and the reconstruction of the internal movement from the external path. Most important is the possibility of applying the model to simulate the movement of this joint for different bone and teeth morphologies. From our knowledge, this is the first time one define the TMJ model with such level of detail. In fact, a model is always a simplification of reality. This work is also a simplification of the complex motion of TMJs but it encompasses the maximum possible real parameters extracted from a volunteer with normal TMJs.

One of the limitations of this work is that examples with real patients with very pathological TMJs were not used in our validation process. We do have some preliminary results on mandible motion from an individual with only one normal TMJ, but the complete analysis is still future work. Other limitation affecting the accuracy of the simulated motion is due to the magnetic process of data capture. The acquired trajectories, for parameterizing the simulation, are usually noisy and have to be filtered before their use in our model. With a possibly smaller influence in the simulation, segmentation of cranium and mandible bones can introduce some inaccuracy. However, we have not investigated the extent of this limitation because we used only a single geometric model coming from an individual. The different models used for validation were obtained by deformation of that one based on cephalometric measures from the two volunteers. Also, since mandible motion path presents small changes even in different masticatory cycles of the same individual, it is very difficult to reproduce exactly the same real motion path during the simulation. We still need to investigate what is the condition (segmentation, 3D model reconstruction or acquired path) that influence most the approximation error. Nevertheless, considering the validation process we performed, the model is a good approximation of real movements. Moreover, since we can take the geometric model and change it according cephalometric measures from living individuals, the model can be used to investigate the relationship of facial morphology and mandibular movement, which is still an open problem [41].

As future works we intend to simulate small mastication movement patterns and analyze how they change based on teeth and food collision. We also intend to work in a complete simulator based on this model to apply it to dentistry education, in orthodontic adjustment of occlusions, or in the planning of craniofacial surgeries to improve post-operative treatment. Through the use of diverse computer graphics techniques, it can also be applied to the physical simulation of muscular forces and soft tissues deformation that involves the mastication system beyond the treatment of collisions

between anatomical structures and foods. The fact of this study requires the definition and the manipulation of variables still ignored in the skull-mandibular research (in contrast to research in other areas of the muscle-skeletal complex) does not reduce its value. On the other way, the work contemplated by this project can become a way to understand its biomechanics role.

Conflict of interest

The authors declare that there is no conflict of interest for this work.

Acknowledgements

The authors would like to thank their collaborators from the Department of Oral and Maxillofacial Surgery, Cliniques Universitaires Saint Luc, Université catholique de Louvain (UCL), Belgium. In particular, we are deeply grateful to Dr. Raphael Olszewski from UCL for fruitful discussions along this work, and Prof. Marcio Lima Grossi from the Post-Graduate Program in Dentistry of the Pontifical Catholic University of Rio Grande do Sul, Brazil, for helping with data acquisition. We are also grateful to the three volunteers that accepted to help us by providing the input data (CTs, MRIs, motion data, and cephalometric measures) for this research.

REFERENCES

[1] R. Olszewski, M.B. Villamil, D.G. Trevisan, L.P. Nedel, C.M. Freitas, H. Reychler, B. Macq, Towards an integrated system for planning and assisting maxillofacial orthognathic surgery, Computer Methods and Programs in Biomedicine 91 (1) (2008) 13–21.

[2] J.J. Lemoine, J.J. Xia, J. Gateno, M.A.K. Liebschner, Radiographic analysis for jaw motion normalization, Journal of Oral Maxillofacial Surgery 63 (2005) 961–967.

[3] J.H. Koolstra, Dynamics of the human masticatory system, Critical Reviews Oral Biology and Medicine 13 (2002) 366–376.

[4] C. Gibbs, T. Meserman, J.B. Reswick, H.J. Derda, Functional movements of the mandible, Journal of Prosthetic Dentistry 26 (1971).

[5] L. Gallo, G. Airoldi, R. Airoldi, S. Palla, Description of mandibular finite helical axis pathways in asymptomatic subjects, Journal Dental Research 76 (2) (1997) 704–713.

[6] D. Ostry, E. Vatikiotis, P.L. Gribble, An examination of the degrees of freedom of human jaw motion in speech and mastication, Journal of Speech, Language, and Hearing Research 40 (1997) 1341–1351.

[7] L. Rubenstein, R.A. Strauss, R. Isaacson, S.J. Lindauer, Quantitation of rotational movements associated with surgical mandibular advancement, The Angle Orthodontist 61 (1991) 167.

[8] V.F. Ferrario, C. Sforza, A. Miani, G. Serrao, J. Tartaglia, Open-close movements in the human temporomandibular joint: does a pure rotation around hinge axis exist? Jornal of Oral Rehabilitation 23 (6) (1996) 401–408.

[9] X. Chen, A comment on: the instantaneous center of rotation during human jaw opening and its significance in interpreting the functional meaning of condylar translation, American Journal Physical Anthropoly 105 (1) (1998) 35.

[10] R. Sadat-Khonsari, C. Fenske, B. Kahl-Nieke, I. Kirsch, H.D. Jüde, Mandibular instantaneous centers of rotation in patients with and without temporomandibular dysfunction, Journal of Orofacial Orthopedics 64 (2003) 256–264.

[11] M. Yatabe, A. Zwijnenburg, C.C. Megens, M. Naeije, Movements of the mandibular condyle kinematic center during jaw opening and closing, Journal of Dentist Research 76 (1997) 714–719.

[12] L.M. Gallo, K. Fushima, S. Palla, Mandibular helical axis pathways during mastication, Journal Dental Research 79 (8) (2000) 1566–1572.

[13] L. Gallo, M. Brasi, B. Ernst, S. Palla, Relevance of mandibular helical axis analysis in functional and dysfunctional TMJS, Journal of Biomechanics 39 (2006) 1716–1725.

[14] J.K. Leader, J.R. Boston, R.E. Debski, T.E. Rudy, Mandibular kinematics represented by a non-orthogonal floating axis joint coordinate system, Journal of Biomechanics 36 (2003) 275–281.

[15] J. Chen, T.R. Katona, The limitations of the instantaneous centre of rotation in joint research, Journal of Oral Rehabilitation 26 (4) (1999) 274–279.

[16] T.P. Sperry, M.J. Steinberg, B.J. Gans, Mandibular movement during autorotation as a result of maxillary impaction surgery, American Journal of Orthodontics 81 (1982) 116.

[17] F. Lepera, Determination of the hinge axis clutches on condyle position, Journal of Prosthetic Dentistry 8 (1958) 260.

[18] P.G. Grant, Biomechanical significance of the instantaneous center of rotation: the human temporomandibular joint, Journal of Biomechanics 6 (1973) 109.

[19] E.D. Rekow, T.M. Speidel, R.A. Koenig, Location of the mandibular center of autorotation in maxillary impaction surgery, American Journal of Orthodontics and Dentofacial Orthopedics 103 (1993) 530.

[20] G. Hellsing, E. Hellsing, S. Eliasson, The hinge axis concept: a radiographic study of its relevance, Journal of Prosthetic Dentistry 73 (1996) 60.

[21] C.W. Spoor, F.E. Veldpaus, Rigid body motion calculated from spatial co-ordinates of markers, Journal of Biomechanics 13 (1980) 391–393.

[22] H.J. Woltring, K. Long, P.J. Osterbauer, A.W. Fuhr, Instantaneous helical axis estimation from 3-d video data in neck kinematics for whiplash diagnostics, Journal of Biomechanics 27 (1994) 1415–1432.

[23] K. Hayashi, R. Delong, I. Mizoguchi, Helical axes of skeletal knee joint motion during running, Journal of Biomechanics 41 (2008) 1632–1638.

[24] A.J. van den Bogert, C. Reinschimidt, A. Lundberg, Comparison of the finite helical axis and the retangular coordinate system in representing orthodontic tooth movement, Journal of Biomechanics 39 (2006) 2925–2933.

[25] A.M.J. Bull, A.A. Amis, Knee joint motion: description and measurement, Proceedings of the I MECH E Part H Journal of Engineering in Medicine 212 (1998) 357–372.

[26] W. Maurel, D. Thalmann, Human sholder modeling including scapulo-thoracic constraint and joint sinus cones, Computer and Graphics 24 (2) (2000) 21–24.

[27] G. Monheit, N.A. Badler, Kinematic model of the human spine and torso, IEEE Computer Graphics and Applications 11 (2) (1991) 29–38.

[28] S.-H. Lee, D. Terzopoulos, Heads up. Biomechanical modeling and neuromuscular control of the neck, in: Proceedings of the ACM SIGGRAPH 2006 Conference, 2006, pp. 1188–1198.

[29] R. Enciso, A. Menon, D.A. Fidaleo, U. Neumann, J. Mah, The virtual craniofacial patient: 3D jaw modeling and animation., Studies in Health Technology and Informatics 94 (2003) 65–71.

[30] K. Fushima, L.M. Gallo, M. Kerbs, S. Palla, Analysis of the TMJ intraarticular space variation: a non-invasive insight during

mastication, J. Medical Engineering and Physics 25 (2003) 181–190.
[31] N. Celebi, E. Carlos Rohner, J. Gateno, P.C. Noble, S.K. Ismaily, J.F. Teichgraeber, J.J. Xia, Development of a mandibular motion simulator for total joint replacement, Journal of Oral and Maxillofacial Surgery 69 (1) (January 2011) 66–79, ISSN 0278-2391, DOI: 10.1016/j.joms.2010.05.085.
[32] A. Maciel, L. Nedel, C. Freitas, Anatomy based joint models for virtual humans skeletons, in: Proceedings of Computer Animation, Geneva, Switzerland, 2002, pp. 110–116.
[33] W. Shao, V. Ng-Thow-Hing, A general joint component framework for realistic articulation in human characters, in: I3D'03: Proceedings of the 2003 Symposium on Interactive 3D Graphics, ACM, New York, NY, USA, 2003, pp. 11–18.
[34] M.B. Villamil, L.P. Nedel, C. Freitas, B. Macq, An anatomy-based approach to simulate the temporomandibular joint movement, in: Proceedings of the 20th International Conference on Computer Animation and Social Agents, Hasselt University, Hasselt, Belgium, 2007, pp. 41–47.
[35] M.B. Villamil, L.P. Nedel, C. Freitas, A. Maciel, A model to simulate the mastication motion at the temporomandibular joint, in: SPIE MEDICAL IMAGING 2005—Physiology, Function, and Structure from Medical Images, vol. 6, San Diego, USA, 2005.
[36] S. Gottschalk, M.C. Lin, D. Manocha, Oobtree: a hierarchical structure for rapid interface detection., in: Proceedings of SIGGRAPH, 1996, pp. 171–180.
[37] T. Saito, J. Toriwaki, New algorithms for euclidian distance transformations of an n-dimensional digitized picture of aplications, Pattern Recoginition 27 (1994) 1551–1565.
[38] O. Cuisenaire, Distance transformation, fast algorithms and applications to medical image processing, Ph.D. thesis, Universite catholique de Louvain, Louvain-la-Neuve, Belgium, 1999.
[39] J.J. Lemoine, J.J. Xia, C.R. Andersen, J. Gateno, W. Buford Jr., M.A.K. Liebschner, Geometry-based algorithm for the prediction of nonpathologic mandibular movement, Journal of Oral and Maxillofacial Surgery 65 (December (12)) (2007) 2411–2417.
[40] U. Posselt, Studies in the mobility of human mandible, Acta Odont. Scandinavica 10 (10) (1952) 19–160.
[41] D.S. Kim, S-J. Hwang, S.-C. Choi, S.S. Lee, M.-S. Heo, K.-H. Heo, W-J. Yi, Quantitative analysis of the TMJ movement with a new mandibular movement tracking and simulation, Korean Journal of Oral and Maxillofacial Radiology (2008) 203–208.